X-ray investigation of subsurface interstitial oxygen at Nb/oxide interfaces

M. Delheusy,[1,2] A. Stierle,[1,a)] N. Kasper,[1] R. P. Kurta,[1] A. Vlad,[1] H. Dosch,[1] C. Antoine,[2] A. Resta,[3] E. Lundgren,[3] and J. Andersen[3]
[1]*Max-Planck-Institut für Metallforschung, Heisenbergstr. 3, 70569 Stuttgart, Germany*
[2]*Commissariat à l'Énergie Atomique, Dapnia/SACM-Centre d'étude Saclay, F-91191 Gif-sur-Yvette Cedex, France*
[3]*Department of Synchrotron Radiation Research, Lund University, 22100 Lund, Sweden*

(Received 22 January 2008; accepted 8 February 2008; published online 11 March 2008)

We have investigated the dissolution of a natural oxide layer on a Nb(110) surface upon heating, combining x-ray reflectivity, grazing incidence diffuse scattering, and core-level spectroscopy. The natural oxide reduces after heating to 145 °C partially from Nb_2O_5 to NbO_2, and an enrichment in subsurface interstitial oxygen by ~70% in a depth of 100 Å is observed. After heating to 300 °C, the oxide reduces to NbO and the surplus subsurface oxygen gets dissolved into the bulk. Our approach can be applied for further investigation of the effect of subsurface interstitial oxygen on the performance of niobium rf cavities. © *2008 American Institute of Physics*.
[DOI: 10.1063/1.2889474]

X-ray free electron lasers and the future International Linear Collider project are based on the performance of niobium superconducting rf cavities for efficient particle acceleration ("cold technology"). High accelerating fields (>30 MV/m) and a low residual resistance of the material are prerequisites for lower running costs; as a result, considerable efforts have been made in the past years to enhance the rf performance of niobium cavities. A remarkable increase of the rf accelerating field has been achieved by low-temperature annealing (below 150 °C for several hours).[1–3] The microscopic origin of this effect has remained unclear; however, it has been argued that a redistribution of subsurface interstitial oxygen within the penetration depth of the rf field into niobium (typically 500 Å) is involved. Interstitial oxygen has, indeed, a strong influence on the conduction properties of Nb, as it decreases the critical temperature for superconductivity by 0.93 K/at. % O.[4,5] From recent core-level spectroscopy experiments on polycrystalline samples[6,7] and Nb(100) single crystals,[8] it was deduced that the oxide layer progressively dissolves upon heating (150–500 °C), with oxygen release into the bulk. High concentrations of interstitial oxygen have been reported at the niobium/oxide interface for Nb(110) films oxidized above 100 °C in air,[9] for a Nb(110) single crystal after high-temperature ultrahigh vacuum (UHV) annealing,[10] and for polycrystalline, high residual resistivity ratio Nb ratio samples in a recent atom probe tomography study.[11] The microscopic mechanism of the oxide layer dissolution and its connection to the formation of subsurface interstitial oxygen are not yet well understood.

In this project, we have carried out detailed *in situ* x-ray investigations on the structure of the oxide layer, its chemical composition, and the formation of subsurface interstitial oxygen for different thermal treatments applied on a Nb(110) single crystal oxidized under atmospheric conditions. For the unambiguous monitoring of subsurface interstitial oxygen, we exploited the fact that interstitial oxygen, which occupies octahedral sites in the niobium lattice, gives rise to strong local distortions of the host lattice,[12] as shown in Fig. 1. Niobium exhibits, as all bcc metals do, an intrinsic instability toward the ω phase, which is manifested in the deep minimum of the phonon dispersion curve at $\mathbf{q}^*=\frac{2}{3}(1,1,1)$. It has been shown that the strong oxygen-induced local lattice distortions couple to this anisotropic softness of the lattice, thereby producing pronounced maxima of the distortion-mediated diffuse x-ray scattering at $\mathbf{q}^*$ [Fig. 3(a)].[13] As we will demonstrate in what follows, the monitoring and quantitative analysis of these diffuse maxima by grazing incidence diffuse x-ray scattering allow us to obtain a detailed picture of the emergence of interstitial oxygen close to the niobium surface.

The Nb(110) single crystals were oriented better than 0.1°, mechanically polished, and subsequently annealed above 2100 °C in UHV.[14] Afterward, the samples were oxidized 6–10 h under ambient conditions. The extended x-ray reflectivity and grazing incidence diffuse x-ray scattering studies were carried out at the MPI-MF beam line at the Angstrmquelle Karlsruhe (ANKA), Germany,[15] at a photon energy of 8.984 keV. The core-level measurements were conducted at the beamline I311 at MAX-Lab in Lund, Sweden.[16] For all studies, the samples were mounted in a dedicated UHV chamber allowing *in situ* annealing [all measurements have been carried out at room temperature (RT)].

We first present the results from x-ray reflectivity and core-level spectroscopy, which provides us with detailed information on the temperature evolution of the different oxide layers. The temperature evolution of the specular x-ray reflectivity and the deduced electron density profiles are shown in Figs. 2(a) and 2(b), respectively. Both sets of data, for the natural oxide formed after 10 h in air at RT and after heating to 145 °C, can be fitted best using a three layer model,[17] which is compatible with a sequence of Nb_2O_5, NbO_2, and NbO, from the surface to the metal/oxide interface. The total thickness of the natural oxide is 20.3 Å, with individual Nb_2O_5, NbO_2, and NbO thicknesses equal, respectively, to 10.2, 6.7, and 3.4 Å (error bar of ±1 Å). The typical interfacial roughness is 2–4 Å.

After heating at 145 °C (5 h, UHV), the total thickness of the oxide has decreased to 18.8 Å. The main effect of the annealing is the reduction of the Nb_2O_5 thickness to 7.9 Å,

a)Electronic mail: stierle@mf.mpg.de.

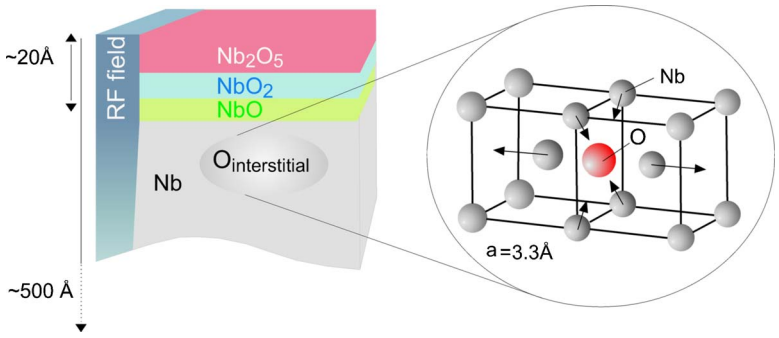

FIG. 1. (Color online) Left: Schematic view of the surface of a niobium single crystal oxidized under ambient conditions, its natural layered oxide, and subsurface interstitial oxygen. For comparison, the penetration depth of the rf field is shown. Right: Niobium lattice distortions in the local neighborhood of interstitial oxygen on octahedral sites (Ref. 12).

leading to a slight thickening of the NbO_2 layer to 7.4 Å. An increase of the Nb_2O_5 electron density by 10% is observed. All interfacial roughnesses stay nearly constant. The oxygen release due to the partial oxide reduction is estimated as ~0.6 ML Nb(110) equivalents. After heating at 300 °C (50 min, UHV), the Nb_2O_5 and NbO_2 layers reduced completely into a 8.6 Å thick NbO layer. This corresponds to an overall oxygen release of ~5 ML equivalents. Complementary grazing incidence x-ray diffraction (not discussed here) confirms the formation of an epitaxial (111) oriented NbO layer.

The Nb 3*d* core-level spectra are shown in Fig. 2(c). The major components are assigned to Nb_2O_5, NbO_2, and NbO located, respectively, at ~5.5, 4, and 1.4 eV (Ref. 18) above the niobium metal binding energy.[8,10,19–21] Additional components from atoms at the interfaces between the different layers are included.[22] Nb_2O_5, the highest and most stable oxidation state of niobium under ambient conditions, predominates for the natural oxide. After heating at 145 °C, the oxide reduces progressively from Nb_2O_5 to NbO_2. At 300 °C, both Nb_2O_5 and NbO_2 decompose nearly entirely into NbO, showing similar behavior as reported on polycrystalline[6,7] and Nb(100) single crystal[8] surfaces. The changes in the core-level spectra are fully consistent with the layer transformations observed by the reflectivity measurements.

We now turn to the study of interstitial oxygen formation. It is known that niobium does not release oxygen in UHV below 1600 °C.[24,25] In turn, oxygen released by the oxide reduction necessarily gets dissolved into niobium across the niobium/oxide interface. For its nondestructive *in situ* detection, we exploit the aforementioned strong diffuse x-ray scattering maxima at $\mathbf{q}^*$ as quantitative fingerprints [see Fig. 3(a)]. Assuming randomly distributed defects with concentration c, the diffuse intensity I_D can be written as $I_D(\mathbf{q}) \propto c(1-c)S(\mathbf{q})$ [$S(\mathbf{q})$ is the square of the scattering amplitude of a single defect], which can be calculated.[12,13] Figure 3(c) shows the measured line scans along the $[1\bar{1}1]$ direction in grazing incidence scattering geometry as a function of the annealing temperature. The glancing angles (incident: 0.31°; exit: 1°) were set to obtain an information depth of ~100 Å.[26,27] These experiments unravel the emergence of diffuse scattering characteristic for the injection of interstitial oxygen into the niobium lattice. In Fig. 3(b), the decomposition of the RT data is plotted. The observed two diffuse maxima arise at the expected $\mathbf{q}^*$ positions. Also visible are additional contributions from epitaxial NbO_2 (Ref. 28) and NbO.[29] The in-plane scans have been fitted using the calculated structure factors for oxygen interstitials[12] and including RT thermal diffuse scattering, the thermal Debye–Waller factor, Compton scattering, and four oxide components taking the NbO_2 and NbO signals into account. The evolution of the diffuse x-ray scattering intensity around $\mathbf{q}^* = \frac{4}{3}(1,\bar{1},1)$ obtained from the fits is shown in Fig. 3(d).

Interestingly, we note that the diffuse intensity increases by ~70% after heating the sample to 145 °C (5 h, UHV),[30] which clearly shows a subsurface interstitial oxygen enrichment within the first 100 Å.[31] From the amount of oxygen released in the first heating step (about 0.6 ML), we can estimate as an upper limit that the average concentration of oxygen within a depth of 100 Å is increasing by ~1.5 at. %.

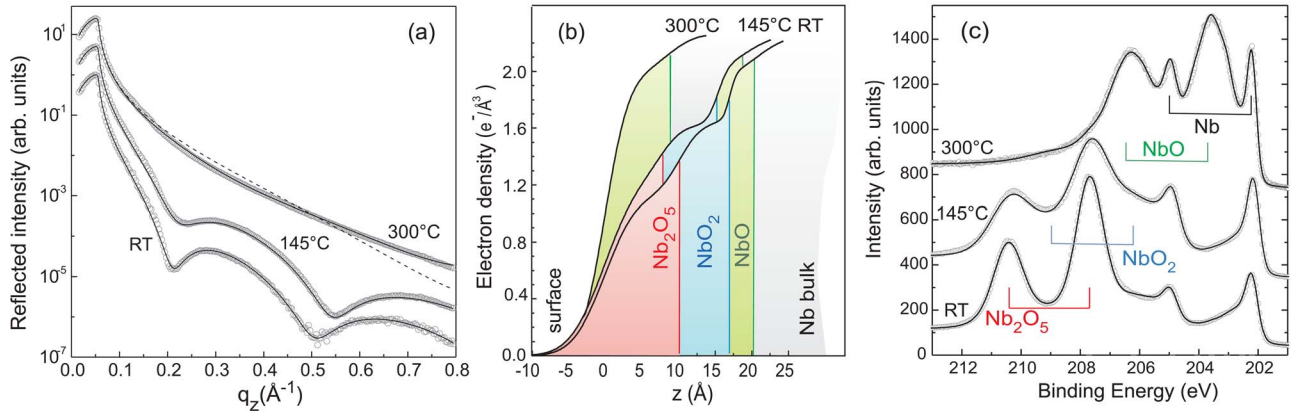

FIG. 2. (Color online) (a) X-ray reflectivity data (open circles) with fits (solid lines) from a Nb(110) single crystal oxidized for 10 h in air at RT, after heating at 145 °C (5 h, UHV) and 300 °C (50 min, UHV). Dashed curve: Best fit of the 300 °C data without oxide layer, which cannot describe the data. (b) Electron density profiles along the surface normal obtained from the fits (see text for details). (c) Core-level Nb $3d_{3/2-5/2}$ spectra (open circles) with fits (solid lines) measured on Nb(110) oxidized for 6 h in air at RT, after 145 °C (3 h, UHV) and 300 °C (30 min, UHV) (photon energy of 650 eV, normal emission angle). In (a) and (c), the scans are offset in the *y* direction.

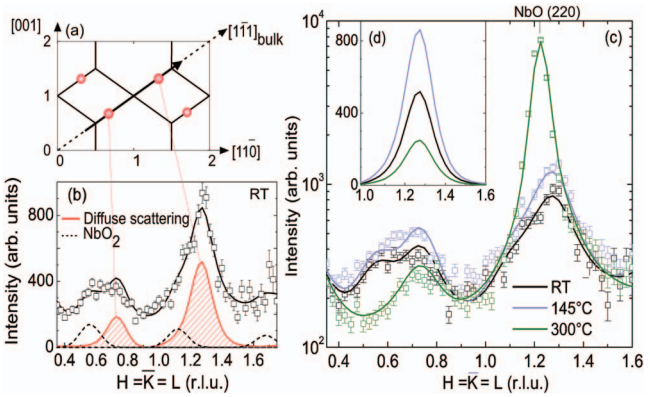

FIG. 3. (Color) (a) Reciprocal space map of the Nb(110) plane: the circles locate the interstitial oxygen-induced diffuse scattering at $\mathbf{q}^*=\frac{2}{3}(1,1,1)$ and equivalent positions. (b) Grazing incidence diffuse scattering measured after RT ambient pressure oxidation along the $[1\bar{1}1]$ direction (open squares: polarization corrected data). The main components of the fit (solid line) are plotted: calculated diffuse peaks around $\mathbf{q}^*=\frac{2}{3}(1,\bar{1},1)$ and $\frac{4}{3}(1,\bar{1},1)$ (red curves); $NbO_2(400)$, (800), and (12 00) peaks (dashed curves). (c) Temperature dependence of the grazing incidence diffuse scattering (open squares) and fits (solid lines), after oxidation for 10 h in air at RT, after heating at 145 °C (5 h, UHV) and at 300 °C (50 min, UHV). (d) Temperature evolution of the interstitial oxygen-induced diffuse intensity around $\mathbf{q}^*=\frac{4}{3}(1,\bar{1},1)$.

At 300 °C, we observe that the NbO_2 signal is not detectable anymore, while the NbO(220) Bragg peak gets very pronounced, both in agreement with the reflectivity and core-level results. In parallel, the diffuse scattering signal from interstitial oxygen is decreasing drastically. We conclude that oxygen gets dissolved by enhanced diffusion into the bulk.[31]

In summary, we have provided a direct insight into the subsurface region of oxidized Nb(110) and its evolution upon heating. We could detect unambiguous scattering signals from subsurface interstitial oxygen, exploiting the diffuse x-ray scattering from the characteristic local lattice distortions occurring around interstitial oxygen defects in niobium. We found that the natural oxide formed after atmospheric pressure oxidation at RT is constituted of Nb_2O_5, NbO_2, and epitaxial NbO. It reduces progressively upon heating, from Nb_2O_5 to NbO_2 at 145 °C and to NbO at 300 °C. After heating to 145 °C, the partial dissolution of the oxide layer leads to a net enrichment of the interstitial oxygen concentration in the first 100 Å underneath the surface. We conclude from this study that the oxygen distribution and its chemical/physical state in the surface and subsurface regime of niobium are highly sensitive to the thermal treatments applied. We have demonstrated that the amount of subsurface interstitial oxygen is a sensible balance between the oxygen release from the oxide reduction and the oxygen diffusion into the niobium bulk. In this work, we have provided a first insight into the interplay between oxide formation/dissolution and the occurrence of interstitial oxygen. We have presented a convenient x-ray technique that can be applied for further investigation of samples prepared under production conditions of niobium rf cavities.

The authors thank R. Henes, A. Weisshardt, A. Weible (sample preparation), and R. Weigel (beam time at ANKA).

[1]B. Visentin, J. P. Charrier, B. Coadou, and D. Roudier, in *Proceedings of the Ninth Workshop on RF Superconductivity, Santa Fe, New Mexico, 1999*, edited by F. Krawczyk (Los Alamos National Laboratory, Santa Fe, NM, 2000), p. 198.
[2]P. Kneisel, in *Proceedings of the Ninth Workshop on RF Superconductivity, Santa Fe, New Mexico, 1999*, edited by F. Krawczyk (Los Alamos National Laboratory, Santa Fe, NM, 2000), p. 328.
[3]G. Ciovati, Appl. Phys. Lett. **89**, 022507 (2006).
[4]C. C. Koch, J. O. Scarbrough, and D. M. Kroeger, Phys. Rev. B **9**, 888 (1974).
[5]W. DeSorbo, Phys. Rev. **132**, 107 (1963).
[6]B. R. King, H. C. Patel, D. A. Gulino, and B. J. Tatarchuk, Thin Solid Films **192**, 351 (1990).
[7]Q. Ma and R. A. Rosenberg, Appl. Surf. Sci. **206**, 209 (2003).
[8]Q. Ma, P. Ryan, J. W. Freeland, and R. A. Rosenberg, J. Appl. Phys. **96**, 7675 (2004).
[9]O. Hellwig, H. W. Becker, and H. Zabel, Phys. Rev. B **64**, 233404 (2001).
[10]I. Arfaoui, C. Cuillot, J. Cousty, and C. Antoine, J. Appl. Phys. **91**, 9319 (2002).
[11]J. T. Sebastian, D. N. Seidman, K. E. Yoon, P. Bauer, T. Reid, C. Boffo, and J. Norem, Physica C **441**, 70 (2006).
[12]H. Dosch, A. V. Schwerin, and J. Peisl, Phys. Rev. B **34**, 1654 (1986).
[13]H. Dosch and J. Peisl, Phys. Rev. B **32**, 623 (1985).
[14]At the end of the heating cycles, the pressure was $\leqslant 10^{-9}$ mbar, which results in an interstitial oxygen concentration of a few ppm.
[15]A. Stierle, A. Steinhäuser, N. Kasper, R. Weigel, and H. Dosch, Rev. Sci. Instrum. **75**, 5302 (2004).
[16]R. Nyholm, J. N. Andersen, U. Johansson, B. N. Jensen, and I. Lindau, Nucl. Instrum. Methods Phys. Res. A **467**, 520 (2001).
[17]L. G. Parratt, Phys. Rev. **95**, 359 (1954); L. Nevot and P. Croce, Rev. Phys. Appl. **15**, 761 (1980).
[18]The NbO peaks shown in Fig. 2(c) include two chemically shifted contributions.
[19]P. C. Karulkar and J. E. Nordman, J. Vac. Sci. Technol. **17**, 462 (1980).
[20]A. Darlinski and J. Halbritter, Surf. Interface Anal. **10**, 223 (1987).
[21]R. Fontaine, R. Caillat, L. Feve, and M. Guittet, J. Electron Spectrosc. Relat. Phenom. **10**, 349 (1977).
[22]The core level spectra were fitted using Doniach–Sunjic line shapes convoluted with Gaussian functions (Ref. 23). Additional depth-resolved information obtained by varying the incident photon energy was included in the analysis (not shown). The spin-orbit splitting was fixed at 2.74 eV and the branching ratio $3d_{3/2-5/2}$ at 0.67.
[23]S. Doniach and M. Sunjic, J. Phys. C **3**, 285 (1970).
[24]E. Fromm and E. Gebhardt, *Gase und Kohlenstoff in Metallen* (Springer, Berlin, 1976), p. 460.
[25]K. Schulze and H. Jehn, Z. Metallkd. **68**, 645 (1977).
[26]H. Dosch, B. W. Batterman, and D. C. Wack, Phys. Rev. Lett. **56**, 1144 (1986).
[27]H. Dosch, Phys. Rev. B **35**, 2137 (1987).
[28]B. O. Marinder, Ark. Kemi **19**, 435 (1962).
[29]A. L. Bowman, T. C. Wallace, J. L. Yarnell, and R. G. Wenzel, Acta Crystallogr. **21**, 843 (1966).
[30]The amount of niobium probed below the oxide for each of the three different treatments is nearly constant due to the changes in thicknesses of the oxide layers present on the surface and their respective optical factors.
[31]Note that the diffusion length of oxygen in bulk niobium during 5 h (50 min) annealing at 145 °C (300 °C) is ~350 Å (~10 000 Å) (Ref. 32).
[32]R. Powers and M. Doyle, J. Appl. Phys. **30**, 514 (1959).